ENGINEERING TRANSACTIONS • *Engng. Trans.* • 40, 3, 313–327, 1992
Polish Academy of Sciences • Institute of Fundamental Technological Research

HOLOINTERFEROMETRIC METHOD FOR STRESS MEASUREMENT IN STRUCTURES

A. KICZKO and S. OCHELSKI (WARSZAWA)

Theoretical foundations of holografic-interferometric method to measure stresses in the civil engineering and mechanical structures are presented. A portable, mountable holographic camera is described. Stress measurement technique and processing of results are described.

1. Introduction

Majority of methods to measure residual stresses are based on the measurements of strain upon unloading or local yielding of material. Commonly used is a method in which unloading holes are drilled and strains are measured with the help of resistance strain gauge rosettes [1]. Blind holes with very small diameters are usually drilled not to disturb an existing stress state too much. Holografic interferometry is used to examine welding stresses in pipes as described in [2] where a method to process results is also offered.

No information on small mountable holographic cameras capable of measuring stresses has been given in the technical literature. Investigations of stresses with the use of holographic interferometry have so far been made in the laboratories. It was model structures or specimens that were mainly examined. The presented holographic camera is small, lightweight and can be easily mounted on a structure under examination. In a single measuring cycle all the three displacement components can be obtained, necessary for the principal stresses and their directions to be found. The camera can furnish fast and accurate assessment of stresses in various structures encountered in civil engineering and machinery. It is especially useful when the surfaces to be examined are moist or excessively rough and strain gauge rosettes cannot be properly placed on such surfaces. Moreover some errors due to a layer of adhesive are eliminated in the holographic method thus supplying more reliable results.

2. Theoretical foundations of the method

Holograms are recorded by illuminating an object with coherent light beams. Interference fringes are registered on a photographic (holographic) plate as a result of interference of two beams: an object beam that carries information on the surface of object and a reference beam (Fig.1). An im-

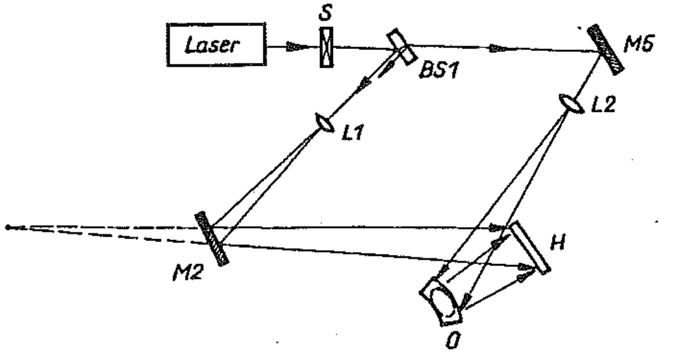

FIG. 1. Hologram registering system: S – shutter, $BS1$ – beam splitter, $M2$, $M5$ – reflecting mirrors, $L1$, $L2$ – microscopic lens, O – object, H – holographic plate.

age is reconstructed by illuminating a hologram with a reproduction light beam that corresponds to the reference beam. The amplitude and phase relations in the virtual image are the same as in an object under study. Double-exposure holography consist in recording two images of an object on one holographic plate, before and after deformation. In the course of reconstruction both images are visible at the same time. The displacements cause a difference in phases between the corresponding points of the images. Provided the displacements are small enough, the two waves interfere with each other and fringes develop indicating the magnitude of displacements, the following relationship is assumed to be valid:

$$\Phi = \bar{K} \circ \bar{d}, \tag{2.1}$$

where $\bar{K}$ is a sensitivity vector bisecting an angle between the illuminating and the viewing directions, $\bar{d}$ denotes a displacement vector of a point. Using notation shown in Fig.2, the following formula can be derived:

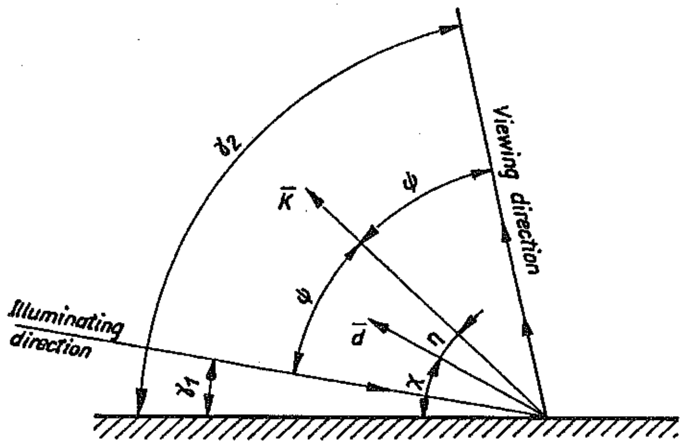

FIG. 2. Displacement components in the plane of interferometer. $\bar{d}$ – displacement vector, $\bar{K}$ – sensitivity vector of the holointerferogram.

$$\Phi = \frac{4\Pi d}{\lambda} \cos\eta \cos\psi , \tag{2.2}$$

where λ is a wavelength of laser light, ψ is an angle included between the sensitivity vector $\bar{K}$ and the viewing or the illumination direction, η is an angle between the vectors $\bar{d}$ and $\bar{K}$. At points for which the phase difference Φ is equal to $(2n+1)\Pi$, where n is a nonnegative integer, the images extinguish completely. Interference fringes are visible at the background of an image. The number n is called an interference fringe order. Between the neighbouring fringes n ceases to be an integer. In what follows another form of the formula (2.2) will be useful, put forward by D.V. NELSON [3]:

$$\Phi = \frac{4\Pi d}{\lambda} \cos\left[\frac{1}{2}(\gamma_1+\gamma_2) - \chi\right] \cos\frac{1}{2}(\gamma_2-\gamma_1) , \tag{2.3}$$

where γ_1 and γ_2 are the angles of illumination and observation directions, respectively, χ is an angle between the displacement vector and a mean plane of an object under examination (Fig.2).

To determine stresses first a shallow blind hole must be drilled and then surface deformations caused by local unloading are measured. Only stresses resulting from elastic strains can be calculated. Their assessment is made with the use of KIRSCH'S [4] analytical solution for a hole throughout a thin plate. To fully analyse the measurement some coefficients are used, derived either experimentally or numerically with the help of the finite elements technique (FET).

Analytical solution concern a thin sheet under uniform stress state in which a hole with the radius r_0 has been drilled. Stress increments due to the presence of the hole are [4]:

$$
\begin{aligned}
\sigma'_r &= \frac{\sigma_1+\sigma_2}{2}\frac{r_0^2}{r^2} + \frac{\sigma_1-\sigma_2}{2}\left(\frac{3r_0^4}{r^4} - \frac{4r_0^2}{r^2}\right)\cos 2\theta\,, \\
\sigma'_\theta &= \frac{\sigma_1+\sigma_2}{2}\frac{r_0^2}{r^2} - \frac{\sigma_1-\sigma_2}{2}\frac{3r_0^4}{r^4}\cos 2\theta\,,
\end{aligned}
\tag{2.4}
$$

where σ_1, σ_2 – principal stresses, θ – an angle between the direction of σ'_r and σ_1, r_0 – hole radius. Average radial strain between the radii r_1 and r_2 amounts to:

$$
\varepsilon_m = \frac{a(1+\nu)}{2E}(\sigma_1+\sigma_2) + \frac{b}{2E}(\sigma_1-\sigma_2)\cos 2\theta\,,
\tag{2.5}
$$

where constants a and b are:

$$
a = -\frac{1}{r_m^2-\delta^2}\,,
\tag{2.6}
$$

$$
b = -(1+\nu)\left[\frac{4}{(1+\nu)(r_m^2-\delta^2)} - \frac{3r_m^2+\delta^2}{(r_m^2-\delta^2)^3}\right],
\tag{2.7}
$$

where, in turn, $\delta = r_2 - r_1$, $r_m = (r_1+r_2)/2$.

In a given radial direction deformations around a hole are symmetric with respect to the hole axis (Fig.3) and therefore a simplifying procedure

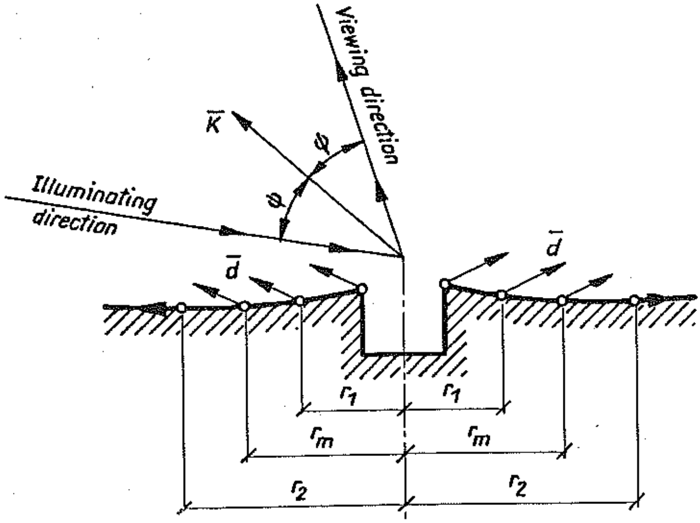

FIG. 3. Deformations around a hole.

for processing interferometric images can be used [3]. Considering two points on the surface lying on a straight line passing through the center of the hole and parallel to the illuminating beam, the displacement projections on the directions of the sensitivity vector are equal to c_1 and c_2 (Fig.4a). Projection of a radial component of the displacement u at both points is equal to c. Thus an average value of the phase difference Φ or the corresponding average order of the interference fringe n is associated with the radial displacement u (Fig.4b).

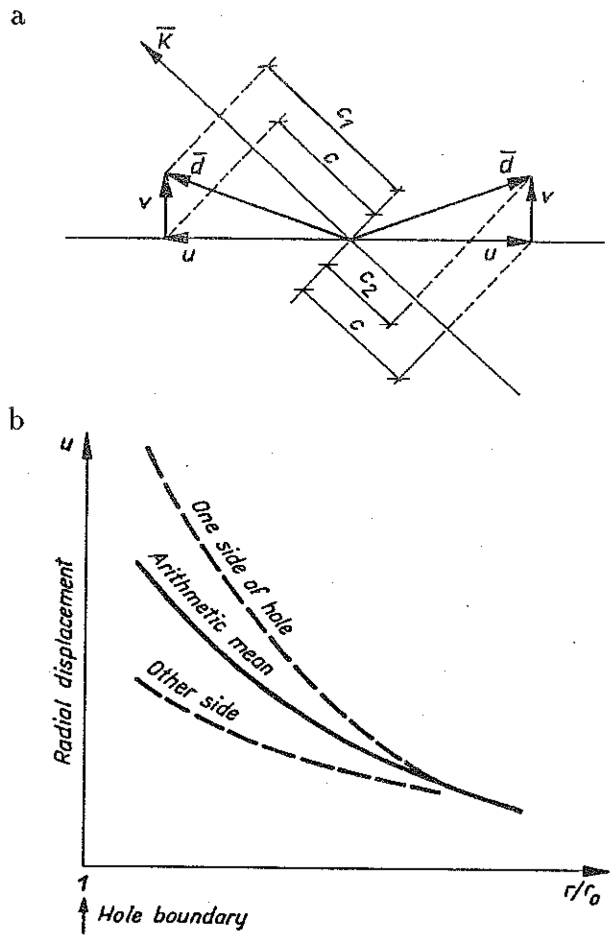

FIG. 4. Geometrical interpretation of the principle of measuring surface displacements.

Complete information on the plane stress state at any point is given by three independent magnitudes σ_1 , σ_2 and θ to be determined. Under some simplifying assumptions the problem can be solved with the use of one hologram only. However, known procedures of this type are either too inaccurate or require involved methods of interference image analysis to be employed [2]. The presented holographic camera, described in some detail in Sec. 3, produces two holointerferograms (by oblique illumination) to measure surface deformations and the third (near-normal illumination) to determine principal stress directions. Radial displacements in the illumination plane are obtained from the oblique light interferograms on which two circles with radii r_1 and r_2 are plotted (Fig.5). The radial displacement Δu_i between

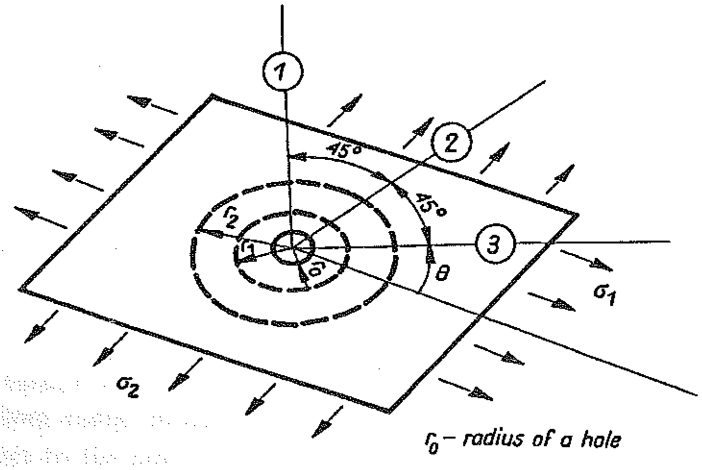

FIG. 5. Directions of measured displacements in the holointerferograms.

the radii r_1 and r_2, in the directions $i = x, y$, and lying on the straight line through the hole center and parallel to the illuminating beam, is determined by means of Eq.(2.3) by inserting $\chi = 0$ and $\Delta\Phi = 2\Pi\Delta n_m$, where n_m denotes the mean value of the change of order of the interference fringe on segments between r_1 and r_2, lying on a straight line through the center of the hole at opposite sides of it, Fig.4b. Thus

$$\Delta u_i = \frac{\lambda(\Delta n_m)_i}{2(\cos\gamma_1 + \cos\gamma_2)} \tag{2.8}$$

while the radial strain is given by

$$\varepsilon_i = \frac{\Delta u_i}{r_2 - r_1} . \tag{2.9}$$

The strain components ε_i in two perpendicular directions $i = x, y$ depend on the principal stresses as follows from the formulae (2.5):

$$
\begin{aligned}
\varepsilon_x &= \frac{a(1+\nu)}{2E}(\sigma_1+\sigma_2) + \frac{b}{2E}(\sigma_1-\sigma_2)\cos 2\theta\,, \\
\varepsilon_y &= \frac{a(1+\nu)}{2E}(\sigma_1+\sigma_2) + \frac{b}{2E}(\sigma_1-\sigma_2)\cos 2(\theta+\Pi/2)\,.
\end{aligned} \tag{2.10}
$$

Once the angle θ and the strains ε_x, ε_y are known, the principal stresses can be calculated by means of

$$
\begin{aligned}
\sigma_1 &= \frac{E(\varepsilon_x+\varepsilon_y)}{2a(1+\nu)} + \frac{E(\varepsilon_x-\varepsilon_y)}{2b\cos 2\theta}\,, \\
\sigma_2 &= \frac{E(\varepsilon_x+\varepsilon_y)}{2a(1+\nu)} - \frac{E(\varepsilon_x-\varepsilon_y)}{2b\cos 2\theta}\,.
\end{aligned} \tag{2.11}
$$

3. Measuring method

A device for measuring stresses with the use of holographic interferometry consist of a holographic camera and a special drill. For computer-aided processing of holograms the system must also comprise a CCD camera, a computer supplied with an image converter, a monitor and a printer. Stresses can be determined to within an accuracy of ± 1 MPa.

To measure displacements near unloading holes in the field conditions, a portable camera is necessary to be mounted on a surface under investigation. A prototype camera has been devised and registered in the Polish Patent Office under the number P286100. The camera makes it possible to measure surface deformations around specially drilled small blind holes that cause local unloading of a small surrounding area during operation of a studied structure. Sufficient information is obtained from one hole to determine magnitudes and directions of principal stresses, similarly as is the case with resistance strain gauges. A light source – a single-mode laser – is firmly fixed to the camera to avoid adjustments of an optical system at every change of its location. The drill is placed between the camera and a surface under study. To achieve sufficient fixity of the holographic system [5], a lightweight and rigid camera had to be devised in order to eliminate any vibrations caused by e.g. wind gusts and thus avoid any phase differences in the interfering beams that would make interferograms useless. The mounting system is integrally built in the camera and surface of the investigated structure forms a part of the holographic interferometer. The camera shown in Fig.6, made of honeycomb sandwich plate and majority of optical instruments are placed inside the box except mirrors (that direct the object beams on a measured surface) and He-Ne laser LGK 7628 (manufactured by Siemens and having the wavelength $\lambda = 632.8\,\mathrm{nm}$ and the power $5\,\mathrm{mW}$ in the basic mode of continuous operation). The laser is characterized by high coherence of radiation, stability of operation and low weight. The continuous operation of the laser is necessary since a certain time must elapse between the drilling of a hole and sufficient cooling of its surroundings.

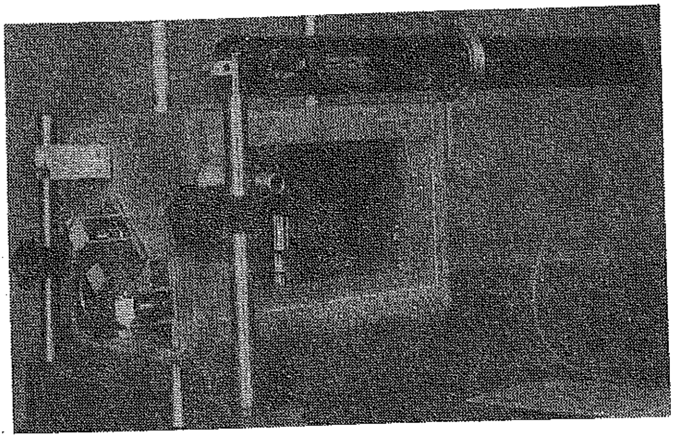

FIG. 6. General view of the camera supplied with 3 interferometers; its side wall is removed.

Special dielectric glass mirrors are used with the thickness 2-3mm. Three interferometers interact with the same holographic plate and an image lens: I1 and I3 are located in the horizontal and vertical planes whereas I2 is inclined at 45°. All the interferometers are illuminated from one laser by means of a system of mirrors. Polarization directions of the object and the reference beams are perpendicular to the plane of each interferometer. Arrangement of the interferometer I3 and splitting of the laser beam are shown in Fig.8 and 7, respectively. Interferometers are located in such a way that the object beams fall on a surface in I1 and I3 at an angle $\gamma_1 \simeq 15°$ (oblique illumination) whereas in I2 they impinge at the incidence angle $\gamma_1 \simeq 75°$ (nearly perpendicular illumination). Such an arrangement makes it possible to obtain in a simple measuring cycle the surface displacements in two

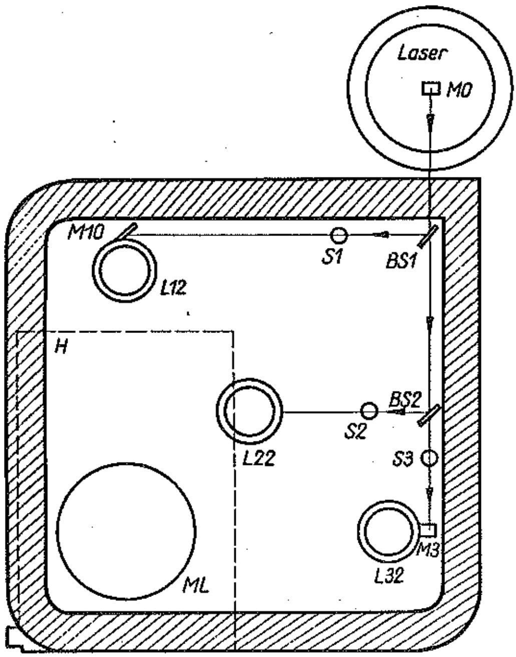

FIG. 7. View of the front side of the camera. Laser light beam is split among 3 interferometers I1, I2, I3. M – mirrors, BS – beam splitters, L – microscopic lenses, ML – magnifying lens, S – shutters, H – holographic plate.

mutually perpendicular directions (I1 and I3) together with the normal displacement (I2) around a hole. He-Ne laser is fixed to the top wall of the camera (Fig.7). The laser beam is reflected from the directional mirror $M0$ and impinges on two beam splitters (semi-transparent mirrors): $BS1$ with transmittance $T = 66$ per cent directs a part of the beam to the interferometer I1, $BS2$ with transmittance $T = 55$ per cent splits the remaining part of the beam between the interferometers I2 and I3. In front of each interferometer a shutter S is placed controlled by means of an electronic clock.

Interferometer I3 (Fig.8) consist of the following elements: a semi-transparent mirror $BS31$ with the transmittance $T = 10$ per cent splits the illuminating light into the reference beam (directed through the mirror $M32$, microscope lens $L31$ and mirrors $M33$, $M34$ on the holographic plate H) and the object beam (directed through a microscopic lens $L32$ and mirror $M35$ on an object under study). The incident light is scattered on the surface of object and directed back to the holographic plate through a magnifying lens ML, common for all the interferometers.

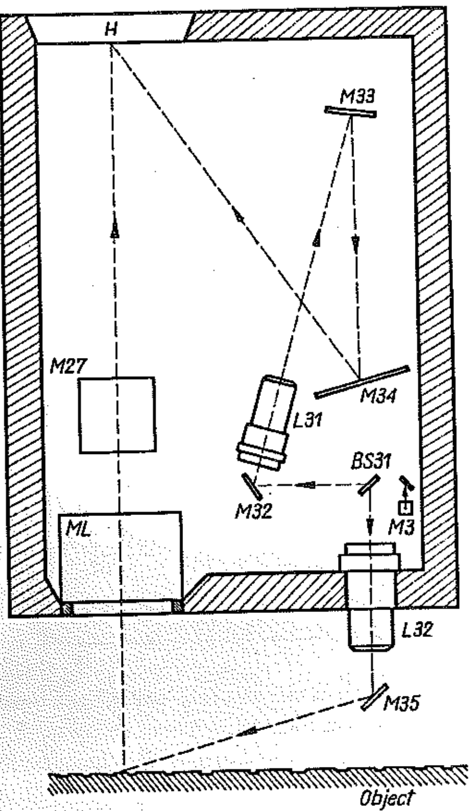

FIG. 8. Set-up of interferometer I3. M – mirrors, BS – beam splitters, L – microscopic lenses, ML – magnifying lens, H – holographic plate.

Holointerferograms from the interferometers I1 and I3 are registered in the lower half of the plate H and from I2 in its upper part. Choice of a sector in which a hologram is to be registered is made with the use of the reference beam. A specially devised electronic clock enables the remote control, with the help of three shutters S, of the order and duration of hologram exposure in particular interferometers. Exposure time can be controlled from 1 to 10 s in a step-wise manner. AGFA-GEWAERT 10E75 holographic plates are used, the standard cassettes being 6×9 cm. The mounting system of the camera consists either of a mechanical set of threaded roots and connectors fixed to the plates glued on the surface of an object or an electromagnetic arrangement powered by batteries. Unloading holes are made with the use of special angle drill; first, a pilot hole with the diameter of 1.5 mm is drilled followed by a suitable reamer to avoid deformations of the walls and lifting of the edge. Prior to measurement, a surface must be cleaned to dispose of all traces of old paint, rust etc. After mounting the camera, the three holograms are illuminated in an arbitrary order and no movements of the camera must be caused. Next, a 1.5 mm drilling bit and a 3 mm reamer are used to make a blind hole 3.6 mm deep. When interferograms with an imposed unmodulated frequency are required, the holographic plate must be rotated before the second illumination of the holograms in the interferometers I1 and I3. After photochemical processing of the holographic plate the image must be suitably analysed to determine the magnitudes and directions of the principal stresses.

4. Analysis of results

The above described measurement method was verified by means of suitable experiments. Validity of assumptions on which the camera was constructed was checked with the help of tests on steel and concrete specimens as well as in the field measurements taken on the underground mining structures. Detailed report and analysis of results is given in [6,7].

Initial analysis of the performance of the camera was made on the laboratory stand by testing a steel specimen with the dimensions $8 \times 60 \times 500$ mm subjected to a uniform uniaxial tension of 100MPa. The next purpose of the experiments was to verify the system of analysis of the produced holointerferograms. The stresses determined by means of an approximate D.V.Nelson's method [3] differed from those applied by 3.2 per cent whereas the stresses obtained by means of the computer-aided analysis if holograms differed by as little as 0.2 per cent.

Residual stresses were investigated at 76 locations in a cast-iron tubing with the dimensions $300 \times 150 \times 150$ mm. Two blind hole-drilling methods were used: in the first one resistant strain gauge rosettes were used, in the other the holographic camera was employed. Some field work was also performed in the pit bottoms of the Bogdanka coal mine. The 960 m level pit was constructed as ribbed steelwork in 1984. Operating conditions were found to be very difficult; together with very high pressure, high humidity caused a considerable corrosion of the structure. As an example holograms are shown in Fig.9 from which the principal stresses $\sigma_1 = -115$ MPa, $\sigma_2 = -89$ MPa were calculated together with the principal direction $\theta = -4°$. Detailed description of the tests can be found in the report [7].

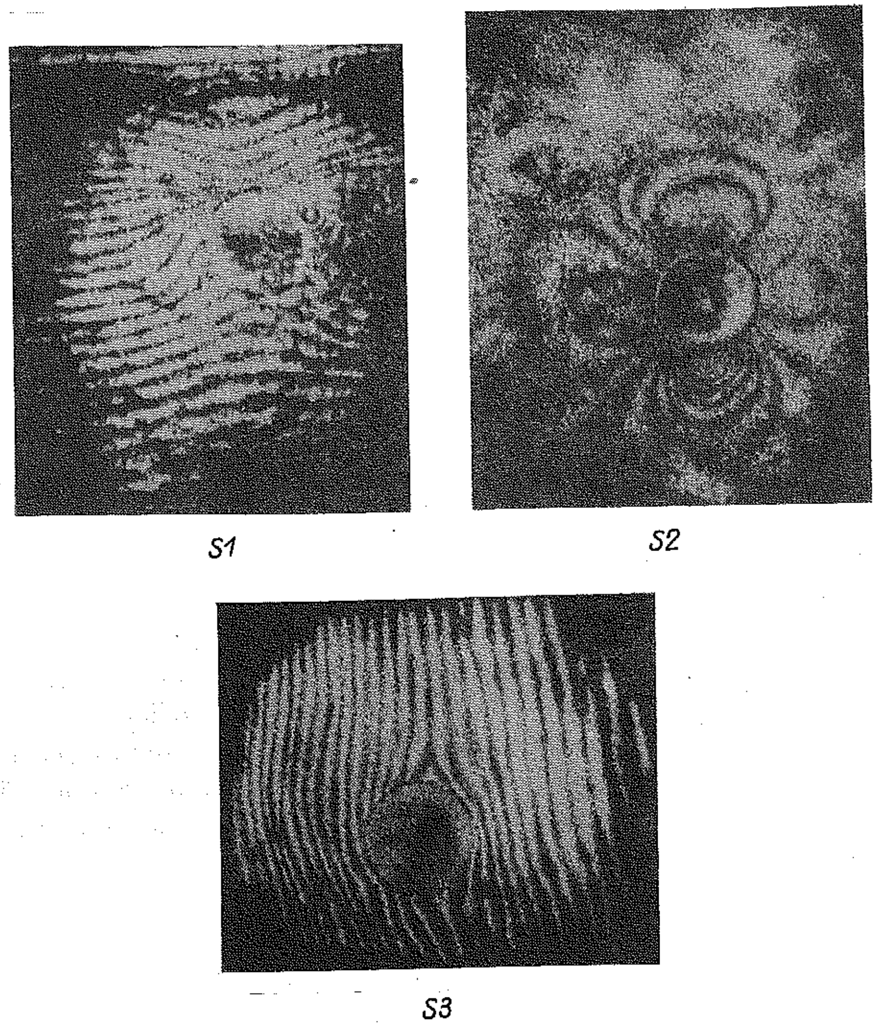

FIG. 9. Holograms obtained from measurements at one point.
I1 and I3 – holointerferograms with the carrier frequency imposed.

As mentioned before, three holointerferograms are required at each selected point of the surface under study. They will be denoted by I1, I2, I3, similarly as the holointerferometers that produced them. Holointerferogram I2 is used to find the principal directions. It can also be employed to assess stress amplitudes in the area of measurements by means of strain maps determined via FEM for various ratios of stresses. Holointerferograms I1 and I3 are used to determine radial displacement components in two mutually perpendicular directions. Radial strains ε_y and ε_x in the planes of interferometers I1 and I3, respectively, can be determined from the corresponding holointerferograms and the principal stresses calculated with the use of Eq.(2.11). Accuracy of measurements largely depends on the accuracy with which the phase difference $\Phi = \Pi \Delta n$ is determined. In practice, the only satisfactory method is the computer-aided image analysis. Three main groups of procedures can be here distinguished [8] based on: localization of fringe extreme [9], discrete phase steps [10] and the double Fourier transform [11, 12].

An analysing program was worked out using the double one-dimensional Fourier transform. First, interferograms are fed into the memory to be analysed in a semi-automatic manner and next the directions and magnitudes of principal stresses are determined. Programs can be run on a PC/AT/386 computer with an image converter that interacts with video camera; PANASONIC F10 was used for the purpose. An important difference is that the holointerferograms I1 and I3 should carry an unmodulated frequency. To this end the measuring procedure was modified in such a way as to obtain the carrier frequency. This was done by means of a small rotation of the holographic plate prior to the second recording of an image. The rotation angle was 0.005 rd. in the plane of each interferometer. The computer-aided method of the holointerferogram analysis required three images (I1, I2, I3) to be fed into the computer memory. Analysis of each of images commences with the determination of a center and radius of the drilled hole by means of an interactive selection of roughly symmetrically situated points belonging to the hole edge. First the interferogram I2 is analysed and the principal direction angle θ is found.

Interferograms I1 and I3 are then used to determine the differences Δn_m in the x- and y-directions, see Eq.(2.8). This value is found with the use of a one-dimensional discrete Fourier transform to analyse suitable segments (64 pixels at each side of the hole at a distance from $2r_0$ to $3r_0$) lying on a straight line that is parallel to the interferometer plane and passes through the center of the hole. Computerized data processing makes it possible to enhance the accuracy of results and to determine the signs of strains [12].

5. Final conclusions

The described holographic camera has proved to be successfully employed in all situations in which small blind holes can be drilled on surfaces of existing structures. Its usefulness has been confirmed in both laboratory and field conditions, as was shown in the examinations of the cast-iron tubings and steel lining of the Bogdanka coal mine pit, respectively. One of the merits of the holographic interferometry is that the measurements can be made irrespective of the quality of a surface under study (deep corrosion, great moisture contest). Thus the measurements of surfaces of concrete structures can be also performed.

The presented holographic camera was constructed as a system of three independent interferometers supplying the principal stress directions and two magnitudes of perpendicular normal stresses on the examined surface. Before the method was established, some experiments had been made to optimize the conditions for the production of holointerferograms and to numerically process the obtained data in order to determine the strain field in the vicinity of an unloading hole. In this manner two material-independent constants a an b were defined that relate the strains and the stresses around the hole. Thus structures made of any materials can be dealt with. The required accuracy of measurements was achieved due to the computer-aided processing of holographic data and due to modifications of interferograms by means of the carrier frequency. The latter enabled signs of strains and stresses to be found as well.

References

1. *Standard test method for Determining Residual Stresses by the Hole-Drilling Strain-Gage Method*, ASTM Standard E847-85.

2. А.А.Антонов, А.И.Бобрик, В.К.Морозов, Г.И.Чернышев, Определеление остаточных напряжений при помощи создания отверствий и голографической интерферометрии, Механика Твердого Тела, No 2, 1980.

3. D.V.Nelson, J.T.McCrikerd, *Residual-stress determination through combined use of holographic interferometry and blind-hole drilling*, Experimental Mechanics, 26, 4, 1986.

4. S.Timoshenko, J.N.Goodier, *Theory of elasticity* [Second edition], McGraw-Hill Book Company, Inc. 1951.

5. R.Pawluczyk, *Holographic experiment technique*, Chapter 2 in Optical Holography [Ed.] M.Pluta [in Polish], PWN 1980.

6. A.Kiczko, *Survey of methods for holographic interferometry as used in the determination of stresses in structures* [in Polish], Doctoral Thesis, Warszawa, WAT, 1991.

7. *Report on the research "Stress state in the lining of gallery 1.2 at the level 960 m in the Bogdanka coal mine"* [in Polish], Warszawa, WAT, 1991.
8. M.Kujawińska, A.Spik, J.Wójcik, *Automatic analyser of fringe images* [in Polish], XIV Symposium on Experimental Methods in Solid Mechanics, Warszawa 1990.
9. M.J.Matczak, T.Pancewicz, J.Stupnicki, *Program "HOLOSTRAIN" as applied to the analysis of strains on cylindrical surfaces* [in Polish], XIII Symposium on Experimental Methods in Solid Mechanics, Warszawa 1988.
10. M.Kujawińska, D.W.Robinson, *Multichannel phase-stepped holographic interferometry*, Applied Optics, 27, 2, 15 January 1988.
11. M.Kujawińska, T.Piątkowski, *Camera analyser of fringe images* [in Polish], XII Symposium on Experimental Methods in Solid Mechanics, Warszawa 1986.
12. D.R.Matthys, T.D.Duddear, J.A.Gilbert, *Automated analysis of holointerferograms for the determination of surface displacement*, Experimental Mechanics, March 1988.

MILITARY TECHNICAL ACADEMY, WARSZAWA.

Received March 6, 1992.